

XCOM: Full Mesh Network Synchronization and Low-Latency Communication for QICK (Quantum Instrumentation Control Kit)

Diego Martin, Luis H. Arnaldi, Kenneth Treptow, Neal Wilcer, Sho Uemura, Sara Sussman, and Gustavo Cancelo*
Fermi National Accelerator Laboratory, Batavia IL, 60510, United States

David I Schuster

Department of Physics and Applied Physics, Stanford University, Stanford CA, 94305

(*cancelo@fnal.gov.)

(Dated: March 20, 2026)

Quantum computing experiments and testbeds with large qubit counts have until recently been a privilege afforded only to large companies [1, 2] or quantum technologies where scaling to hundreds or thousands of qubits does not require a substantial increase in quantum control hardware (neutral atoms [3, 4], trapped ions [5], or spin defects [6]). Superconducting and spin qubit testbeds critically depend on scaling their control systems beyond what a single electronics board can provide. Multi-board control systems combining RF, fast DC control, bias, and readout require precise synchronization and communication across many hardware and firmware components. To address this, we present XCOM, a network that synchronizes QICK boards [7, 8] and the absolute clocks governing quantum program execution to within 100 ps, free of drift and loss of lock. XCOM also provides deterministic, all-to-all simultaneous data communication with latency below 185 ns. Like QICK itself, XCOM is compatible with a broad range of qubit technologies and is designed to scale to large systems.

I. INTRODUCTION

Among today’s successful qubit technologies, superconducting qubits are notable for requiring a very high hardware I/O count [9]. Silicon spin qubits and quantum dots are also very demanding in the number of fast DC bias outputs required to manipulate spins and perform readout [10, 11]. Quantum hardware continues to evolve at a rapid pace. Control systems need to be flexible, while also providing high performance and complex functionality. FPGAs continue to be at the center of modern control systems; in particular, RF-FPGAs help integrate analog RF acquisition and generation of signals up to 10 GHz with high-speed parallel logic, minimizing hardware footprint and power consumption [12]. In the future, ASICs will take over some of the functions of today’s room-temperature electronics, but they still need to overcome several challenges. Modern RF-FPGAs such as the AMD RF-SoC integrate high-speed DACs, ADCs, and programmable logic in a single device, a level of complexity and reconfigurability that cryo-CMOS ASICs have yet to match. We expect that for the next 5 to 10 years, room-temperature FPGAs and discrete component electronics will continue to drive the ecosystem [13].

In order to minimize physical channel count, QICK has achieved 8- and 16-channel frequency multiplexing. This is successfully used for multi-qubit readout [8]. Multiplexing of qubit control remains a qubit device challenge. Today, most proprietary, commercial, and open-source control systems map from a few up to 16 signal generator outputs (plus inputs) to a single FPGA. It is clear that larger qubit systems require control hardware expansion, hosting multiple FPGAs, DACs, ADCs, bias circuits, I/O, and computer interface ports (e.g., Ethernet, USB, etc.). Furthermore, most systems requiring multi-piece hardware platforms also require the hardware pieces to be synchronized and to support communication. In this publication, we describe XCOM, a syn-

chronization and low-latency message exchange bus with a mesh network topology. Multi-module hardware communication is available in most modern quantum control systems. For instance, Xu et al. at LBNL have reported a comprehensive list of control systems that support synchronization and communication at some level [14]. In particular, the QubiC project [15] and the Manarat project [16] use the AMD RF-SoC FPGAs and ZCU216 evaluation boards that are also the hardware foundation of QICK [17].

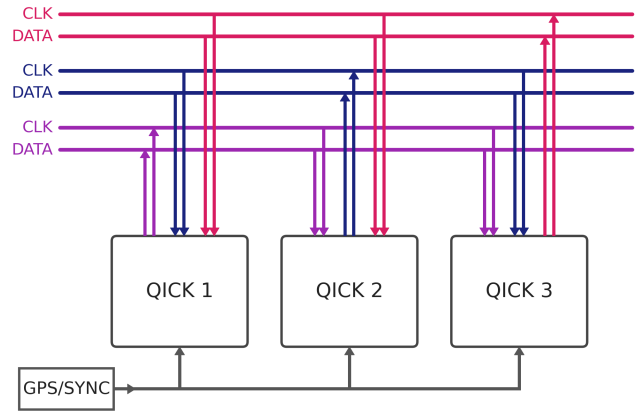


FIG. 1: XCOM block diagram. Each QICK board connects a $Tx_{data/clk}$ output to a pair of LVDS lines. Three $Tx_{data/clk}$ channels are shown in purple, blue, and red. All boards have $Rx_{data/clk}$ inputs to listen to all $Tx_{data/clk}$ channels. A shared GPS/SYNC reference (bottom) provides the external clock common to all boards.

II. ARCHITECTURE OVERVIEW

Each QICK board runs its own timed-processor (tProc), which maintains a 48-bit absolute clock counter used to time all quantum program execution (i.e. the experiment clock domain). While all boards share the same clock frequency, their absolute counters are not inherently aligned. This misalignment has direct consequences for multi-board experiments: for instance, a pulse command issued simultaneously on two different boards will not produce temporally aligned output pulses unless the absolute clocks on both boards have been synchronized. XCOM is designed to solve this problem.

The XCOM architecture is a full mesh network as shown in Figure 1. There are as many data channel/clock pairs as there are QICK boards connected to the network. Each board is the sole speaker on its own channel, while all boards listen on all channels. This parallel architecture allows point-to-point and broadcast messages to occur concurrently on different channels. Received messages are stored in memory and handled by the XCOM peripheral IP firmware block as described in Section IV. Prior to synchronization, each board is assigned a network ID number, which can be set by software or auto-assigned by the XCOM.

To synchronize the network, one board is designated the master. The master is allowed to broadcast reset, start, and stop commands to the absolute clocks of all boards, aligning every tProc to the same counter value and enabling precise cross-board pulse timing. Since all XCOM interfaces and firmware IPs are identical, any board can be assigned the master role in software. Board frequency synchronization is based on an external reference source (e.g., a rubidium clock), and a single broadcast from the master is sufficient to synchronize all absolute time counters across the network simultaneously. The board synchronization is required to happen a single time, when the XCOM network is configured or when a new node is added to the network.

III. HARDWARE IMPLEMENTATION

The XCOM hardware consists of two components: a small transceiver board plugged into the FMC connector of the ZCU216 board (Figure 2a), and a single external hub to fan out Tx drivers from each board to Rx receivers in all boards (Figure 2b). The current hardware prototype supports up to five RFSoc boards, while the XCOM firmware IP already supports up to 15 boards and can be extended further; a larger hardware prototype is straightforward to build.

The XCOM maps a single $Tx_{data/clock}$ from each board to 5 $Rx_{data/clock}$ in all boards. To minimize FPGA logic and data latency, we implement a separate clock per Tx driver. We choose this option over the one that embeds clock and data on a single LVDS line, because the latter requires extracting and synchronizing the transmitter clock to the receiver clock, adding more logic and latency.

XCOM uses LVDS high performance (HP) I/O from the FPGA routed to the FMC connector. The small XCOM Tx/Rx board plugs onto the FMC and uses the TI DS90LV804 LVDS

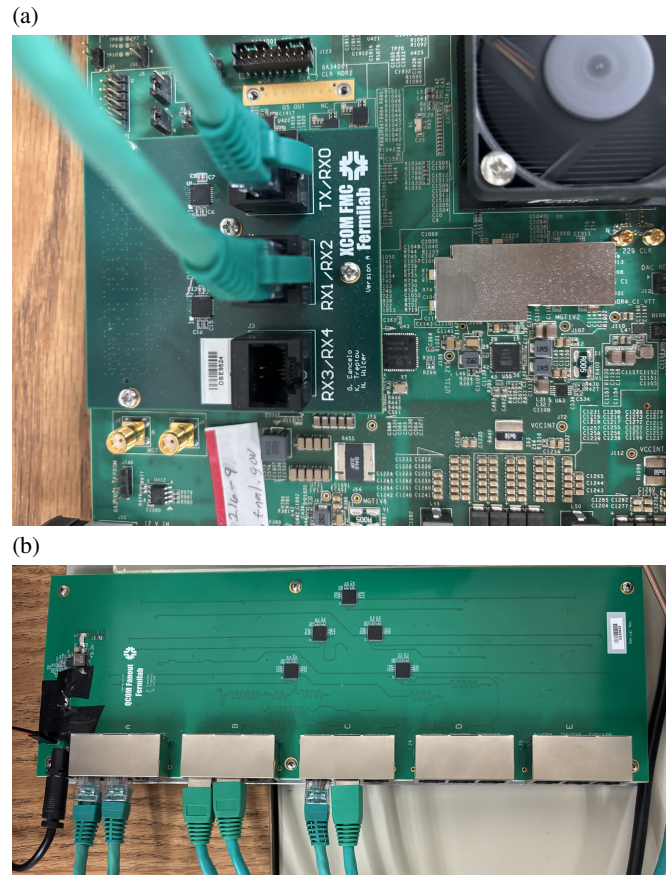


FIG. 2: XCOM hardware. (a) Transceiver board mounted on the RFSoc FMC connector, providing one $Tx_{data/clock}$ driver and five $Rx_{data/clock}$ receivers via three RJ45 connectors. One such board is required per QICK board in the network. (b) Standalone fanout hub, which distributes each incoming $Tx_{data/clock}$ pair to five $Rx_{data/clock}$ output pairs, one per board in the network.

quad-drivers capable of driving 60mA at 800Mb/s to bring the HP I/Os to the three RJ45 female connectors as shown in Figure 2a. Each connector carries 2 LVDS data channels and 2 LVDS clock pairs (e.g., $DATA_0$, CLK_0 pair; $DATA_1$, CLK_1 pair). The LVDS $Tx_{data/clock}$ pairs are input to the XCOM hub, which uses TI LMK1D2108 buffers to fan out each pair to output $Rx_{data/clock}$ signals routed back to the FMC board on each QICK board as shown in Figure 2b.

Figure 3 shows the block diagram of the XCOM fanout hub. Each Tx_i ($i = 0, \dots, 4$) originates from a different RFSoc board and enters the hub, where it is copied by fanout buffer FO_i into five outputs. Each fanned-out output is routed to one Rx_i on each board. Note that Tx_i and Rx_i blocks sharing the same color reside on the same RFSoc FMC transceiver board (Figure 2a).

The FPGA HP I/O LVDS supports up to 312.9 MHz. For this prototype, we have initially set the clock to 100 MHz and used both clock edges to sample data, achieving 200 Mb/s. The clock speed will be pushed to 300 MHz to reduce the cur-

rent 32-bit word latency from 186 ns to 62 ns.

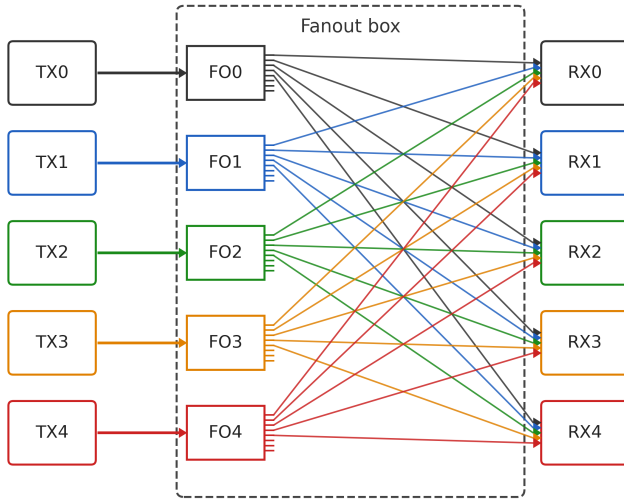


FIG. 3: Block diagram of the XCOM fanout hub. Each Tx_i ($i = 0, \dots, 4$) originates from a different RFSoc board and is copied five times by fanout buffer FO_i . Each output is routed to one Rx_i on a board in the network. Tx_i and Rx_i blocks sharing the same color reside on the same RFSoc FMC transceiver board (Figure 2a).

IV. SYNCHRONIZATION PROTOCOL

The QICK main firmware components, as shown in Figure 4, are the Signal Generators, the Readouts, the tProc, and peripherals such as digital I/O and the XCOM. The Signal Generators (SG) and Readouts (RD) have been described in [8] and [7]. SGs and RDs support multi-tone multiplexing of up to 16 tones and DDS up/down frequency conversion from DC–10 GHz. They can generate pulses with arbitrary I-Q envelopes of variable length, modulating a carrier whose frequency, phase, and amplitude can be updated every fabric clock cycle (2.4 ns) or as frequently as needed. The readouts support several types of filters and averages for two or more detection levels. The tProc runs the compiled quantum program that dispatches events to SGs, manages peripherals, and receives status and/or data from RDs. The tProc runs at the experiment’s absolute clock and is able to execute multiple nested loops and conditional jumps for control and feed-forward. The XCOM allows multiple boards to be frequency- and phase-synchronized to an external reference, and allows multiple tProcs to synchronize to the same absolute clock. The absolute time is a 48-bit register associated with every tProc on every board. That absolute time can be started, stopped, or reset by the tProc, the software, or by an external input (I/O). The absolute clock wraps around after approximately 8 days, and does so without interrupting ongoing experiments. To synchronize PLLs, SGs, RDs, I/Os, and tProc absolute timing, we do the following:

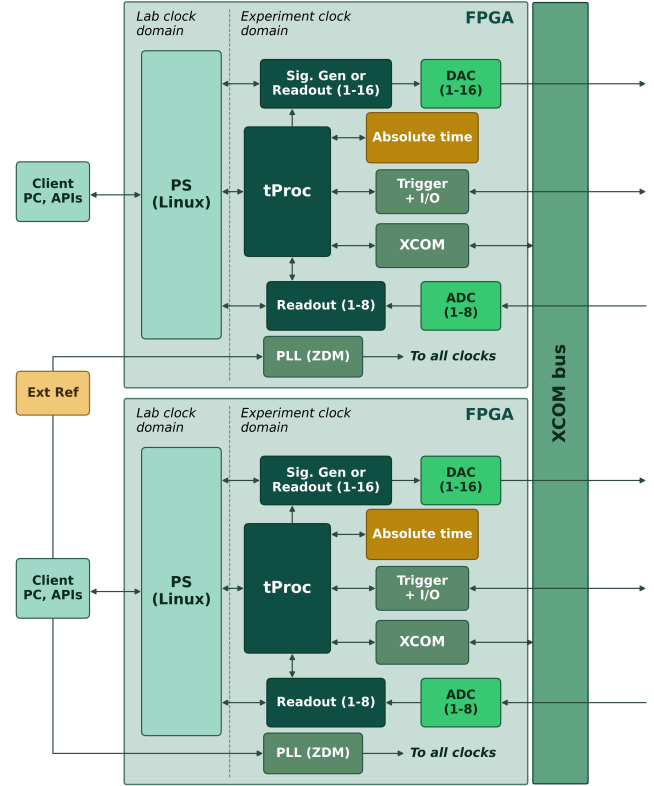


FIG. 4: QICK firmware block diagram. Two QICK firmware FPGA blocks (light green) are shown, each connected to a shared external stable reference and to the XCOM parallel bus. Each firmware block contains up to 16 Signal Generators (SG, with up to $16 \times$ frequency multiplexing), up to 8 Readouts (RD, with up to $8 \times$ frequency multiplexing), 16 digital I/O channels, and peripherals including the XCOM. Each block has a dedicated tProc and absolute time clock. The DACs and ADCs are internal to the RFSoc FPGA and communicate with the logic blocks at up to 10 GS/s and 2.5 GS/s, respectively. All blocks operate in the experiment clock domain. The QICK firmware communicates with the FPGA’s built-in quad-core ARM processor (PS) and through it to the client PC.

- Connect the TI LMK04828B PLLs of all RFSoc boards to a stable external reference using matched-length cables.
- Configure and lock the LMK04828B on each board using the nested zero delay (ZDM) mode. The ZDM guarantees that all PLL outputs will have the same phase across all boards with sub-picosecond jitter.
- Synchronize all DAC blocks and ADC blocks on each board using the FPGA multi-tile sync (MTS) calibration. MTS uses PLL output clocks and SYSREF to synchronize DAC and ADC tiles. Each tile groups 4 DAC blocks or ADC blocks. For instance, MTS guarantees that DAC outputs will align to within 1 DAC sample



FIG. 5: Oscilloscope traces of three RF waveforms from three different QICK boards and one PMOD digital I/O signal, all triggered simultaneously via matched-length cables. The PMOD drivers are bandwidth-limited, showing a 1.5 ns rise time. The inset shows a timing skew of only 20 ps between the three RF channels, demonstrating sub-100 ps cross-board synchronization. Achieving this level of synchronization requires PLL nested zero-delay mode lock on each board, multi-tile synchronization (MTS) across DAC and ADC tiles within each board, and absolute clock alignment across all boards via XCOM.

time. For a 10 GHz clock, this represents a maximum skew of 100 ps on a single board and also across multiple boards.

Figure 5 shows three RF waveforms from three different QICK boards and one PMOD digital I/O signal, all triggered simultaneously via matched-length cables. The PMOD drivers are bandwidth-limited, showing a 1.5 ns rise time. As shown in the inset, the timing skew between the three RF channels is only 20 ps, demonstrating sub-100 ps cross-board synchronization. This result is achieved through the combination of PLL nested zero-delay mode lock on each board, multi-tile synchronization (MTS) across DAC and ADC tiles, and absolute clock alignment across all boards via XCOM.

V. OPERATION AND VALIDATION

The XCOM can be operated directly from the PS side (e.g., Python notebooks) or from the tProc, with its synchronization and communication functions embedded as part of the quan-

tum algorithm. When operated from a Python script, some additional latency is introduced, intrinsic to an API running in a Linux environment; in that case the XCOM interface uses the FPGA AXI. When managed by the tProc, commands and data exchange run at the fabric clock (currently 430 MHz), achieving the lowest latency.

The XCOM is managed by the tProc as a peripheral. Any algorithm in Python (or C++, etc.) can use the QICK tProc classes and functions, which are compiled into assembly machine language, loaded into the tProc program memory, and run independently at the absolute time clock frame [7]. The tProc XCOM classes, defined and integrated into the peripheral driver, provide commands to configure boards on the XCOM network, control the tProc state on other boards, and exchange data.

During network configuration, one board is designated the master and all others act as slaves. Since all XCOM interfaces and IPs are equal, any board can be assigned that role in software. A one-time XCOM power-up and synchronization sequence proceeds as follows, assuming every board is already synchronized to an external reference and, optionally,

calibrated using MTS as described in Section IV:

- Each board gets a network ID by running the AUTO-ID protocol. The protocol identifies the network port number and assigns it as the XCOM-ID for that board.
- The master board broadcasts a RESET absolute clock command to synchronize.
- The master board broadcasts a START absolute clock command. All tProcs begin running at the same time.

Once the network is running, any board can exchange data with any other board or broadcast to all boards. Data sizes are 8, 16, 32 bits, each preceded by a 4-bit board address field and a 4-bit command field. Communication latency is deterministic: 186 ns per 32-bit word at the current prototype clock of ~ 100 MHz. Since the HP LVDS I/O and XCOM drivers support up to 312.9 MHz, a factor of 3 faster, latency can be reduced to about 62 ns per 32-bit word with a modification to the logic that runs the SERDES transceivers. The XCOM also provides a single flag bit, the fastest available message type, useful for point-to-point configurations such as a token ring network; this feature will be expanded in the future to be useful for a full mesh network.

The following validation tests have been performed on the XCOM prototype:

- **Synchronization stability:** The XCOM was synchronized and configured once. Lock stability and tProc synchronization have been tested to remain free of drift or loss of lock for multiple days.
- **Long-term deterministic latency:** 100K messages

were exchanged between 2 and 3 boards with identical latency over a loopback path.

- **Conditional software jumps:** Wait for a message and jump based on received data.

VI. CONCLUSION AND FUTURE WORK

We have presented XCOM, a synchronization and low-latency communication network for QICK boards. The results shown are from a first prototype supporting up to five boards, operating at a clock speed below the maximum supported rate. The prototype successfully demonstrates the XCOM protocol in a real hardware environment, achieving a 32-bit word latency of 186 ns that can be reduced to 62 ns with a simple firmware modification. The prototype supports simultaneous exchange of multiple messages without central control, and sub-picosecond timing and phase synchronization have been demonstrated across three boards.

The current hardware design is not final; a more compact implementation is feasible for larger systems. XCOM enables control systems requiring accurate synchronization and communication, facilitating tasks such as auto-calibration of larger qubit systems with assistance from a central AI agent [18, 19], as well as QEC syndrome detection with low-level decoders [20, 21].

In the future, the QICK team will continue developing deterministic, low-latency inter-board communication systems that scale without bottlenecks to high-speed control of large qubit systems. In the near term, we will port and expand XCOM to the AMD Versal RF platform [13].

[1] R. Acharya, D. A. Abanin, L. Aghababaie-Beni, I. Aleiner, T. I. Andersen, M. Ansmann, F. Arute, K. Arya, A. Asfaw, N. Astrakhantsev, J. Atalaya, R. Babbush, D. Bacon, B. Ballard, J. C. Bardin, J. Bausch, A. Bengtsson, A. Bilmes, S. Blackwell, S. Boixo, G. Bortoli, A. Bourassa, J. Bovaird, L. Brill, M. Broughton, D. A. Browne, B. Buchea, B. B. Buckley, D. A. Buell, T. Burger, B. Burkett, N. Bushnell, A. Cabrera, J. Campero, H.-S. Chang, Y. Chen, Z. Chen, B. Chiaro, D. Chik, C. Chou, J. Claes, A. Y. Cleland, J. Cogan, R. Collins, P. Conner, W. Courtney, A. L. Crook, B. Curtin, S. Das, A. Davies, L. De Lorenzo, D. M. Debroy, S. Demura, M. Devoret, A. Di Paolo, P. Donohoe, I. Drozdov, A. Dunsworth, C. Earle, T. Edlich, A. Eickbusch, A. M. Elbag, M. Elzouka, C. Erickson, L. Faoro, E. Farhi, V. S. Ferreira, L. F. Burgos, E. Forati, A. G. Fowler, B. Foxen, S. Ganjam, G. Garcia, R. Gasca, É. Genois, W. Giang, C. Gidney, D. Gilboa, R. Gosula, A. G. Dau, D. Graumann, A. Greene, J. A. Gross, S. Habegger, J. Hall, M. C. Hamilton, M. Hansen, M. P. Harrigan, S. D. Harrington, F. J. H. Heras, S. Heslin, P. Heu, O. Higgott, G. Hill, J. Hilton, G. Holland, S. Hong, H.-Y. Huang, A. Huff, W. J. Huggins, L. B. Ioffe, S. V. Isakov, J. Iveland, E. Jeffrey, Z. Jiang, C. Jones, S. Jordan, C. Joshi, P. Juhas, D. Kafri, H. Kang, A. H. Karamlou, K. Kechedzhi, J. Kelly, T. Khaira, T. Khattar, M. Khezri, S. Kim, P. V. Klimov, A. R. Klots, B. Kobrin, P. Kohli, A. N. Korotkov,

F. Kostritsa, R. Kothari, B. Kozlovskii, J. M. Kreikebaum, V. D. Kurilovich, N. Lacroix, D. Landhuis, T. Lange-Dei, B. W. Langley, P. Laptev, K.-M. Lau, L. Le Guevel, J. Ledford, J. Lee, K. Lee, Y. D. Lensky, S. Leon, B. J. Lester, W. Y. Li, Y. Li, A. T. Lill, W. Liu, W. P. Livingston, A. Locharla, E. Lucero, D. Lundahl, A. Lunt, S. Madhuk, F. D. Malone, A. Maloney, S. Mandrà, J. Manyika, L. S. Martin, O. Martin, S. Martin, C. Maxfield, J. R. McClean, M. McEwen, S. Meeks, A. Megrant, X. Mi, K. C. Miao, A. Mieszala, R. Molavi, S. Molina, S. Montazeri, A. Morvan, R. Movassagh, W. Mruczkiewicz, O. Naaman, M. Neeley, C. Neill, A. Nersisyan, H. Neven, M. Newman, J. H. Ng, A. Nguyen, M. Nguyen, C.-H. Ni, M. Y. Niu, T. E. O'Brien, W. D. Oliver, A. Opremcak, K. Ottosson, A. Petukhov, A. Pizzuto, J. Platt, R. Potter, O. Pritchard, L. P. Pryadko, C. Quintana, G. Ramachandran, M. J. Reagor, J. Redding, D. M. Rhodes, G. Roberts, E. Rosenberg, E. Rosenfeld, P. Roushan, N. C. Rubin, N. Saei, D. Sank, K. Sankaragomathi, K. J. Satzinger, H. F. Schurkus, C. Schuster, A. W. Senior, M. J. Shearn, A. Shorter, N. Shutty, V. Shvarts, S. Singh, V. Sivak, J. Skrzny, S. Small, V. Smelyanskiy, W. C. Smith, R. D. Somma, S. Springer, G. Sterling, D. Strain, J. Suchard, A. Szasz, A. Sztein, D. Thor, A. Torres, M. M. Torunbalci, A. Vaishnav, J. Vargas, S. Vdovichev, G. Vidal, B. Villalonga, C. V. Heidweiller, S. Waltman, S. X. Wang, B. Ware, K. Weber, T. Weidel, T. White, K. Wong, B. W. K. Woo, C. Xing, Z. J.

- Yao, P. Yeh, B. Ying, J. Yoo, N. Yosri, G. Young, A. Zalcman, Y. Zhang, N. Zhu, and N. Zobrist, *Nature* **638**, 920–926 (2024).
- [2] M. AbuGhanem, *The Journal of Supercomputing* **81** (2025), 10.1007/s11227-025-07047-7.
- [3] M. Kornjača, H.-Y. Hu, C. Zhao, J. Wurtz, P. Weinberg, M. Hamdan, A. Zhdanov, S. H. Cantu, H. Zhou, R. A. Bravo, K. Bagnall, J. I. Basham, J. Campo, A. Choukri, R. DeAngelo, P. Frederick, D. Haines, J. Hammett, N. Hsu, M.-G. Hu, F. Huber, P. N. Jepsen, N. Jia, T. Karolyshyn, M. Kwon, J. Long, J. Lopatin, A. Lukin, T. Macri, O. Marković, L. A. Martínez-Martínez, X. Meng, E. Ostroumov, D. Paquette, J. Robinson, P. S. Rodriguez, A. Singh, N. Sinha, H. Thoreen, N. Wan, D. Waxman-Lenz, T. Wong, K.-H. Wu, P. L. S. Lopes, Y. Boger, N. Gemelke, T. Kitagawa, A. Keesling, X. Gao, A. Bylinskii, S. F. Yelin, F. Liu, and S.-T. Wang, (2024), arXiv:2407.02553 [quant-ph].
- [4] B. Zhang, G. Liu, G. Bornet, S. P. Horvath, P. Peng, S. Ma, S. Huang, S. Puri, and J. D. Thompson, “Leveraging erasure errors in logical qubits with metastable ^{171}Yb atoms,” (2025), arXiv:2506.13724 [quant-ph].
- [5] S.-A. Guo, Y.-K. Wu, J. Ye, L. Zhang, W.-Q. Lian, R. Yao, Y. Wang, R.-Y. Yan, Y.-J. Yi, Y.-L. Xu, B.-W. Li, Y.-H. Hou, Y.-Z. Xu, W.-X. Guo, C. Zhang, B.-X. Qi, Z.-C. Zhou, L. He, and L.-M. Duan, *Nature* **630**, 613–618 (2024).
- [6] M. Cambria, S. Chand, C. M. Reiter, and S. Kolkowitz, *Phys. Rev. X* **15**, 031015 (2025).
- [7] L. Stefanazzi, K. Treptow, N. Wilcer, C. Stoughton, C. Bradford, S. Uemura, S. Zorzetti, S. Montella, G. Cancelo, S. Sussman, A. Houck, S. Saxena, H. Arnaldi, A. Agrawal, H. Zhang, C. Ding, and D. I. Schuster, *Rev. Sci. Instrum.* **93**, 044709 (2022).
- [8] C. Ding, M. Di Federico, M. Hatridge, A. Houck, S. Leger, J. Martinez, C. Miao, D. S. I. L. Stefanazzi, C. Stoughton, S. Sussman, K. Treptow, S. Uemura, N. Wilcer, H. Zhang, C. Zhou, and G. Cancelo, *Phys. Rev. Res.* **6**, 013305 (2024).
- [9] Castelveccchi, *Nature* **81** (2023), 10.1038/d41586-023-03854-1.
- [10] A. J. Weinstein, M. D. Reed, A. M. Jones, R. W. Andrews, D. Barnes, J. Z. Blumoff, L. E. Euliss, K. Eng, B. H. Fong, S. D. Ha, D. R. Hulbert, C. A. C. Jackson, M. Jura, T. E. Keating, J. Kerckhoff, A. A. Kiselev, J. Matten, G. Sabbir, A. Smith, J. Wright, M. T. Rakher, T. D. Ladd, and M. G. Borselli, *Nature* **81** (2023), 10.1038/s41586-023-05777-3.
- [11] H. C. George, M. T. Mądzik, E. M. Henry, A. J. Wagner, M. M. Islam, F. Borjans, E. J. Connors, J. Corrigan, M. Curry, M. K. Harper, D. Keith, L. Lampert, F. Luthi, F. A. Mohiyaddin, S. Murcia, R. Nair, R. Nahm, A. Nethewala, S. Neyens, B. Patra, R. D. Raharjo, C. Rogan, R. Savytskyy, T. F. Watson, J. Ziegler, O. K. Zietz, S. Pellerano, R. Pillarisetty, N. C. Bishop, S. A. Bojarski, J. Roberts, and J. S. Clarke, *Nano Letters* **25**, 793–799 (2024).
- [12] AMD, “Amd Zynq Ultrascale+ RFSocS,” <https://www.amd.com/en/products/adaptive-socs-and-fpgas/soc/zynq-ultrascale-plus-rfsoc.html> (2020).
- [13] AMD, “Amd Versal RF Series,” <https://www.amd.com/en/products/adaptive-socs-and-fpgas/versal/rf-series.html> (2025).
- [14] Y. Xu, A. D. Rajagopala, N. Fruitwala, and G. Huang, “Multi-fpga synchronization and data communication for quantum control and measurement,” (2025), arXiv:2506.09856 [quant-ph].
- [15] Y. Xu, G. Huang, J. Balewski, R. Naik, A. Morvan, B. Mitchell, K. Nowrouzi, D. I. Santiago, and I. Siddiqi, “Qubic: An open source fpga-based control and measurement system for superconducting quantum information processors,” (2021), arXiv:2101.00071 [quant-ph].
- [16] A. Silva and A. Orgaz-Fuertes, “Manarat: A scalable qick-based control system for superconducting quantum processors supporting synchronized control of 10 flux-tunable qubits,” (2025), arXiv:2507.10676 [quant-ph].
- [17] “Zynq Ultrascale+ RFSOC Product Data Sheet: Overview (DS889),” https://www.xilinx.com/support/documentation/data_sheets/ds889-zynq-usc-rfsoc-overview.pdf (2020).
- [18] S. Li, J. M. Miller, P. J. Lee, G. Andersson, C. R. Conner, Y. J. Joshi, B. Karimi, A. M. King, H. L. Malc, H. Mishra, H. Qiao, M. Ryu, X. Wu, S. Xing, H. Yan, J. Shi, and A. N. Cleland, “Large language model-assisted superconducting qubit experiments,” (2026), arXiv:2603.08801 [quant-ph].
- [19] V. Sivak, A. Morvan, M. Broughton, R. G. Cortiñas, J. Bausch, A. W. Senior, M. Neeley, A. Eickbusch, N. Shutty, L. A. Beni, J. S. Spencer, F. J. H. Heras, T. Edlich, D. Abanin, A. Abbas, R. Acharya, G. Aigeldinger, R. Alcaraz, S. Alcaraz, T. I. Andersen, M. Ansmann, F. Arute, K. Arya, W. Askew, N. Astrakhantsev, J. Atalaya, B. Ballard, J. C. Bardin, H. Bates, A. Bengtsson, M. B. Karimi, A. Bilmes, S. Bilodeau, F. Borjans, A. Bourassa, J. Bovaird, D. Bowers, L. Brill, P. Brooks, D. A. Browne, B. Buchea, B. B. Buckley, T. Burger, B. Burkett, N. Bushnell, J. Busnaina, A. Cabrera, J. Campero, H.-S. Chang, S. Chen, B. Chiaro, L.-Y. Chih, A. Y. Cleland, B. Cochrane, M. Cockrell, J. Cogan, R. Collins, P. Conner, H. Cook, W. Courtney, A. L. Crook, B. Curtin, M. Damyanov, S. Das, D. M. Debroy, S. Demura, P. Donohoe, I. Drozdov, A. Dunsworth, V. Ehimhen, A. M. Elbag, L. Ella, M. Elzouka, D. Enriquez, C. Erickson, V. S. Ferreira, M. Flores, L. F. Burgos, E. Forati, J. Ford, A. G. Fowler, B. Foxen, M. Fukami, A. W. L. Fung, L. Fuste, S. Ganjam, G. Garcia, C. Garrick, R. Gasca, H. Gehring, R. Geiger, Élie Genois, W. Giang, D. Gilboa, J. E. Goeders, E. C. Gonzales, R. Gosula, S. J. de Graaf, A. G. Dau, D. Graumann, J. Grebel, A. Greene, J. A. Gross, J. Guerrero, L. L. Guevel, T. Ha, S. Habegger, T. Hadick, A. Hadjikhani, M. C. Hamilton, M. P. Harrigan, S. D. Harrington, J. Hartshorn, S. Heslin, P. Heu, O. Higgott, R. Hiltermann, H.-Y. Huang, M. Hucka, C. Hudspeth, A. Huff, W. J. Huggins, E. Jeffrey, S. Jevons, Z. Jiang, X. Jin, C. Joshi, P. Juhas, A. Kabel, D. Kafri, H. Kang, K. Kang, A. H. Karamlou, R. Kaufman, K. Kechedzhi, T. Khattar, M. Khezri, S. Kim, C. M. Knaut, B. Kobrin, F. Kostritsa, J. M. Kreikebaum, R. Kudo, B. Kueffler, A. Kumar, V. D. Kurilovich, V. Kutsko, N. Lacroix, D. Landhuis, T. Lange-Dei, B. W. Langley, P. Laptev, K.-M. Lau, J. Ledford, J. Lee, K. Lee, B. J. Lester, W. Leung, L. Li, W. Y. Li, M. Li, A. T. Lill, W. P. Livingston, M. T. Lloyd, A. Locharla, L. D. Lorenzo, D. Lundahl, A. Lunt, S. Madhuk, A. Maiti, A. Maloney, S. Mandrà, L. S. Martin, O. Martin, E. Mascot, P. M. Das, D. Maslov, M. Mathews, C. Maxfield, J. R. McClean, M. McEwen, S. Meeks, K. C. Miao, Z. K. Mineev, R. Molavi, S. Molina, S. Montazeri, C. Neill, M. Newman, A. Nguyen, M. Nguyen, C.-H. Ni, M. Y. Niu, L. Oas, R. Orosco, K. Ottosson, A. Pagano, A. D. Paolo, S. Peek, D. Petteerson, A. Pizzuto, E. Portoles, R. Potter, O. Pritchard, M. Qian, C. Quintana, A. Ranadive, M. J. Reagor, R. Resnick, D. M. Rhodes, D. Riley, G. Roberts, R. Rodriguez, E. Ropes, L. B. D. Rose, E. Rosenberg, E. Rosenfeld, D. Rosenstock, E. Rossi, P. Roushan, D. A. Rower, R. Salazar, K. Sankaragomathi, M. C. Sarihan, K. J. Satzinger, M. Schaefer, S. Schroeder, H. F. Schurkus, A. Shahingohar, M. J. Shearn, A. Shorter, V. Shvarts, S. Small, W. C. Smith, D. A. Sobel, B. Spells, S. Springer, G. Sterling, J. Suchard, A. Szasz, A. Szein, M. Taylor, J. P. Thiruraman, D. Thor, D. Timucin, E. Tomita, A. Torres, M. M.

- Torunbalci, H. Tran, A. Vaishnav, J. Vargas, S. Vdovichev, G. Vidal, C. V. Heidweiller, M. Voorhees, S. Waltman, J. Waltz, S. X. Wang, B. Ware, J. D. Watson, Y. Wei, T. Weidel, T. White, K. Wong, B. W. K. Woo, C. J. Wood, M. Woodson, C. Xing, Z. J. Yao, P. Yeh, B. Ying, J. Yoo, N. Yosri, E. Young, G. Young, A. Zalcman, R. Zhang, Y. Zhang, N. Zhu, N. Zobrist, Z. Zou, R. Babbush, D. Bacon, S. Boixo, Y. Chen, Z. Chen, M. Devoret, M. Hansen, J. Hilton, C. Jones, J. Kelly, A. N. Korotkov, E. Lucero, A. Megrant, H. Neven, W. D. Oliver, G. Ramachandran, V. Smelyanskiy, and P. V. Klimov, “Reinforcement learning control of quantum error correction,” (2026), arXiv:2511.08493 [quant-ph].
- [20] N. Liyanage, Y. Wu, S. Tagare, and L. Zhong, *IEEE Transactions on Quantum Engineering* **5**, 1–18 (2024).
- [21] N. Liyanage, Y. Wu, E. Houghton, and L. Zhong, “Network-integrated decoding system for real-time quantum error correction with lattice surgery,” (2025), arXiv:2504.11805 [quant-ph].